International Journal of Pure and Applied Mathematics
Volume 81 No. 3 2012, 439-461
ISSN: 1311-8080 (printed version)
url: http://www.ijpam.eu
ijpam.eu

PROPAGATION OF LOCAL AND GLOBAL SMOOTHED PERIODIC WAVES IN A SPRING-BLOCK MODEL

Kodwo Annan
Department of Mathematics & Computer Science
Minot State University
Minot, North Dakota, 58707, USA

Abstract: The global conditions under which a spring-block model coupled with friction force depicting a seismic fault are studied. Existence and stability conditions of the wave solutions exhibited by smoothed and non-smoothed versions of the friction force are proved analytically. Runge-Kutta numerical scheme is used to scan the parameter value space of the system. Both analytical and numerical solutions presented allowed us to gain more insight of the wave solution developed. The insight gained has important implications for the understanding of earthquakes and other dissipative driven systems.

Key Words: spring-block, earthquakes, friction, solitons, existence

1. Introduction

Numerous observations of slow slip transients in the earth crust have been reported in various tectonic locations [1-3] and geothermal areas [4],[5]. Even though earthquakes are complex phenomena, the fundamental physical idea is stick-slip fracture instability of a fault driven by slow steady motions of tectonic plates [6]. An earthquake event is defined as a cluster of block that slips due to the initial slip of a single block. One of the standard models used to describe such phenomenon is the spring-block model [7]. The model

Received: August 9, 2012

represents earth's crust as a coupled system of driven oscillators where non-linearity occurs through a stick-slip frictional instability. Simulation of the spring-block model consists of N blocks of the same mass m, each connected by elastic springs of same strength k_c driven by a load plate moving at very low velocity v. The blocks also feel the effect of the loading plate through a series of leaf spring of stiffness k_l. All blocks are subjected to friction force which may be decreasing with increasing speed (velocity-weakening force) or dependent on relative velocity and interface state.

Initially, any block is stuck to the ground as long as the total elastic force acting on it is less than the static friction threshold. Once the static friction is exceeded, a sliding block experiences a dynamic friction force F_N that varies inversely stresses into neighboring blocks causing them to subsequently move. When the moving blocks stops, we call this as the completion of one event.

Since its introduction, different variations of spring-block model have received much attention [5, 7-9] and have given insight about earthquake faults and other dissipative driven systems. For example, Carlson and Langer used one-dimensional version of the model to identify i) microscopic events with maximum velocities less than the moving speed which tends to smoothened the in-homogeneities in the system, ii) localized events with velocities larger than the pulling speed, and iii) delocalized events with velocities far larger than the localized events and accompanied by fractures that propagated at the order of the speed of sound [8]. Further studies on a similar model by Schmittbuhl et al. (1993) showed that these fractures spanned the entire system with solitary wave solutions when periodic boundary conditions are satisfied [9]. In the perspective of the solitary waves, many of the models were found to be chaotic for a large range of physical parameters. One of the most commonly used parameters in interpreting such chaotic waves has been the friction law.

Burridge and Knopoff incorporated a friction term in their model to investigate earthquakes and found to be dependent on the block's velocity [7]. However, further studies later indicated that the friction term could not be the single valued function of the velocity [10]. Daub and Cralon (2007) studied fault-scale behavior of various friction laws and discussed their implications for dynamic rupture and earthquake faults [12]. However, due to the non-linear term, analytic integration could not be established even for the simplest case when only one block was used.

A thorough analysis of simplified forms of the friction term was proposed by Carlson and Langer [13-14] who obtained both analytical solutions and stability conditions in the continuous limit at the onset of the slip instability. However, recent studies [15] have raised questions regarding the existence and the stability of the wave propagation solutions. Other researchers have used [11-13] extremely small time steps to help solve the nonlinear problem. In Lapusta and Rice (2003), for example, the authors regularize the nonlinear friction term for values near zero [11]. This was done by either allowing rate values to be of either sign or taking absolute values or by linearizing the friction term in a small interval. However, the chaotic nature of the model was rarely observed in the simulation even with realistic parameters. Thus, either these numerical alteration of the friction term lack better solution algorithms or the way the friction term affected solitary waves development in spring-block models were not fully understood.

In this paper, both analytical and numerical solutions of a fully nonlinear spring-block model are considered. A velocity-weakening friction force proposed by Carlson and Langer [13] would be the only nonlinearity term in the system that would be responsible for the instability that generates chaotic behavior. The purpose of this work is in two-fold: i) to prove the existence of solitary waves in the spring-block system in a limit of weak coupling between the blocks and ii) to scan the space of parameters as the stiffness ratio is increased using a Runge-Kutta numerical scheme with fixed time step.

After the description of the model formulation in the next section, we give Local and Global existence proofs for both uncoupled and coupled Spring-Block problems in Sections 3 and 4. Numerical simulations and analysis of our model presentation are given in Section 5. We finally conclude in Section 6.

2. Model Formulation

If $X_i(t^*)$ is the displacement of the i-th block at time t^*, then the equation for the periodic traveling wave solution X_i in the moving blocks for $t = i + t^*/\tau$ are given by

$$\frac{m}{\tau^2}\ddot{X}_i = k_c(X_{i+1} - 2X_i + X_{i-1}) - k_p X_i - F_N(v + \frac{\dot{X}_i}{\tau}), \qquad (1)$$

where F_N is the non-linear velocity-dependent friction force, v is the constant velocity of the moving block, and τ^{-1} is the velocity of the traveling wave. Equation (1) involves Differential Inclusion which has its route in optimal control theory and Advance-and Delay problems. From the equation, as long as the total elastic force on each block is less than the static friction threshold, the block is stuck in its place. Once the static friction threshold is exceeded, motion in the i-th block occures. We introduce the following characteristic quantities:

- $\omega = \sqrt{\frac{k_p}{m}}$; Frequency of the block attached to the spring of the driving plate
- F_0; Normalized friction force
- $L = \frac{F_0}{k_p}$; Maximum horizontal length of the spring before block slips neglecting elastic forces.
- $t_0 = \frac{T}{2\pi} = \omega^{-1}$; Time, were T is the period of the block attached to a spring.
- $v_0 = \frac{L}{t_0} = \frac{2\pi L}{T} = L\omega$; Characteristic velocity that determines the scale of the friction force
- $\ell^2 = \frac{k_c}{k_p}$; is the characteristic elastic coefficient

Then, the dimensionless quantities for displacement, time, speed and friction force are respectively:

- $u_i = \frac{X_i}{L} \Rightarrow X_i = \frac{F_0 u_i}{k_p}$,
- $t = \frac{t^*}{t_0} \Rightarrow t^* = \frac{t}{\omega}$,
- $V = \frac{v}{v_0} = \frac{v}{L\omega} \Rightarrow v = VL\omega$,
- $F = \frac{F_N}{F_0}$; which is the dimensionless friction force working at the i-th block.

Thus, the dimensionless form of equation (1) becomes

$$\frac{\ddot{x}_i}{\tau^2} = \ell^2(x_{i+1} - 2x_i + x_{i-1}) - x_i - F(V + \frac{\dot{x}_i}{\tau}). \tag{2}$$

The dimensionless equation (2) reveals that the model behavior is controlled by two main parameters: the stiffness ratio ℓ, and the strength of the velocity-weakening V. We numerically investigate the effect of varying ℓ in Section 5. However, the stability and the existence of uncoupled and coupled versions of equation (2) are presented in the next two sections.

3. Local and Global Existence of Uncoupled Problem

To prove the existence of the periodic solution for the uncoupled smoothed equation (2) for any value of $\tau = \tau_0 \in \mathbb{R}^+$ we set $\ell = 0$, scale time as $t\tau$, and define a smoothed friction force F_ε that approximates the non-smooth friction force F. Thus (2) becomes

$$\ddot{x} + x + F_\varepsilon\,(V + \dot{x}) = 0. \tag{3}$$

We first claim that Hopf bifurcation leads to periodic orbit and prove the claim.

Definition 3.1. A periodic orbit of a continuous dynamical system $\mho$ is a set of the form.

$$\{\Omega(t,p)\,|t\in[0,T]\,\} \tag{4}$$

where T and p are respective time and point satisfying $\Omega(t,p)=p$. If the set is singleton, then the periodic orbit is said to be generating.

Rewriting equation (3) in Hamiltonian form gives

$$\dot{X}=H_\varepsilon(X)=\begin{pmatrix}0 & 1\\ -1 & 0\end{pmatrix}X+\begin{pmatrix}0\\ -F_\varepsilon(V+\dot{x})\end{pmatrix}, \tag{5}$$

where $X=\begin{pmatrix}x\\ \dot{x}\end{pmatrix}$ and $X_e=\begin{pmatrix}-F_e(V)\\ 0\end{pmatrix}$ as the only equilibrium point. If we consider a positive parameter $V\in[v_{0,}\infty)$ where $v_{0,}$ is close to zero and approaches zero as $\varepsilon\to\infty$ then the two conjugate eigenvalues which crosses the imaginary axis when $F'_\varepsilon(V)=0$ are

$$\lambda=\frac{-F'_\varepsilon(V)\pm i\sqrt{-\Delta}}{2}. \tag{6}$$

Consider the existence of solution in the neighborhood of the equilibrium point for V close to a critical value V_c. Then $\delta=V-V_c$ where $V_c>v_0$ is the only positive real number y such that $F'_\varepsilon(y)=0$. Thus, at $\delta=0$ we have $F''_\varepsilon(V_c)\neq 0$. Hence Hopf bifurcation can be applied and stable periodic wave is established since the isolated pair of the complex eigenvalues crosses the imaginary axes.

Theorem 3.2. *Let V_c be the unique solution in $\mathbb{R}^+$ for $F'_\varepsilon(y)=0$ and define a bifurcation parameter $\delta=V-V_c$, then*

(i) For small and positive δ, the equilibrium is unstable, but stable periodic orbit of radius $\sqrt{\delta}$ is established in the neighborhood of the equilibrium.

(ii) For small and negative δ, the equilibrium is stable and there is no periodic orbit in the neighborhood of the equilibrium.

Remark 3.3. Bifurcation analyses [16] have shown that there exists a periodic orbit in the neighborhood of the equilibrium point when $\delta\approx 0$ and positive. Thus the theorem gives asymptotic stability for the periodic orbit when $\delta\approx 0$.

To prove that global existence of the periodic orbit hold for all $\delta>0$, we state and prove theorem 3.4.

Theorem 3.4. *For all $V > V_c$ and all $\tau_0 \in \mathbb{R}^+$ there exists a periodic orbit for the equation (7).*

$$\frac{\ddot{x}}{\tau_0^2} + x + F_\varepsilon\left(V + \frac{\dot{x}}{\tau_0}\right) = 0. \tag{7}$$

The global behavior of bounded trajectories of differential equation (7) in the plane (i.e. of a time independent vector field, f) have a deceptively simple beautiful structure given by the Poincare-Bendixson theorem which we state and prove after the following definitions and lemmas:

Definition 3.5. If $C = C(t)$ is a trajectory of a time independent vector field, we define the $\omega-limit$ set of C^1, denoted by $\omega(C)$, to consist of all points p such that there exists a sequence $t_n \to \infty$ as $C(t_n) \to p$

Definition 3.6. If S is a line segment in $\mathbb{R}^2$ and $p_1, p_2, p_3, ...$ are (possible finite) sequence of points lying on S, then the sequence is monotone on S if $(p_i - p_{i-1}) \cdot (p_2 - p_1) \geq 0$ for every $i \geq 2$.

Definition 3.7. A (possible finite) sequence $p_1, p_2, p_3, ...$ of points on a trajectory C of a domain Ω is said to be monotone on C if we can choose a point p and times $t_1 \leq t_2 \leq ...$ such that $\Omega(t_i, p) = p_i$ for each i.

Definition 3.8. A transversal of Ω is a line segment S such that f is not tangent to S at any point of S.

By a transverse line segment we mean a closed line segment contained in Ω, so that f is not parallel to the line segment at any point of the segment. Thus the vector field points are consistent to one side of the segment. Clearly, any non-equilibrium point of Ω is in the interior of some transverse line segment.

In particular, f does not vanish at any point of S. If $f(A) \neq 0$ for $A \in \omega(C)$, we can always find a transversal to f passing through A. Let choose a subspace of codimension one of the tangent space at A which does not contain $f(A)$, and then choose a surface tangent to this subspace at A. Then at all points sufficiently near to A the vector field f will not be tangent to this surface on account of continuity. Thus, f points towards one of the two sides at A, and hence by continuity must point to the same side at all points of the transversal. In other words, all trajectories cross the transversal in the same direction.

Lemma 3.9. *The set $\omega(C)$ is closed and invariant under the flow generated by f.*

Proof. Suppose that $\{A_n\}$ is a sequence of points in $\omega(C)$ which converge to a point A. We can find a sequence in times $\{t_n\}$ such that $t_n > n$ and

$d(C(t_n), A_n) < n^{-1}$ where d denotes distance. Then $C(t_n) \to A$, thus proving that $\omega(C)$ is closed.

To prove that $\omega(C)$ is invariant, suppose that $A \in \omega(C)$ and let $D(t)$ be the trajectory through A with $D(0) = A$. Let $\{t_n\} \to \infty$ be a sequence with $C(t_n) \to A$,. Define $C_n(t) = C(t + t_n)$ so that C_n is a reparametrization of the trajectory C with $C_n(0) \to A$. Then for any fixed t, the continuous dependence of solutions of differential equations upon initial conditions implies that $C_n(t) \to D(t)$. Thus, proving that $D(t) \in \omega(C)$. $\square$

Lemma 3.10. *For any bounded interval $[a, b]$ a trajectory C can cross the transversal, S, at most a finite number of times for $a < t < b$.*

Proof. Suppose the contrary. We would then have an infinite sequence of times $a < t < b$ with $C(t_n) \in S$. By passing to a subsequence, we may assume that the t_n converge to some point $s \in [a, b]$. Thus the points $C(t_n)$ lie on S and converge to $C(s) \in S$. If more than one of the points $C(t_n)$ coincides with $C(s)$, then C is a periodic trajectory, of some minimal period. It cannot be the case that infinitely many of the points t_n have $C(t_n) = C(s)$, because the difference between each successive such t_n has to be a multiple of the minimal period, and so these infinitely many $t_n{}'s$ could not lie in the bounded interval $[a, b]$. So in all cases, we will have infinitely many of the t_n with $C(t_n) \neq C(s)$. Thus, we find a collection of secants (in local coordinates) $\overline{C(t_n) \cdot C(s)}$ whose limiting direction is tangent to C, but is also tangent to S, a contradiction. $\square$

Lemma 3.11. *Let A be a point of a transversal, S. For every $\varepsilon > 0$, there is a neighborhood N of A such that every trajectory, C with $C(0) \in N$ intersects S at some time t with $|t| < \varepsilon$.*

Proof. Let $C(x_0, y_0, t)$ denote the trajectory which passes through (x_0, y_0) at $t = 0$, and let $Y(x_0, y_0, t)$ be the y coordinate of $C(x_0, y_0, t)$. Then, transversality says that $y'(0, 0, 0) > 0$. By the implicit function theorem, the equation $Y(x_0, y_0, t) = 0$ has a unique continuous solution $t(x_0, y_0)$ with $|t| < \varepsilon for (x_0, y_0)$ in some neighborhood of the origin. $\square$

Lemma 3.12. *Suppose $\omega(C)$ contains a point A with $f(A) \neq 0$. If S is a transversal segment through A, then there exists a monotone sequence of times $t_n \to \infty$ such that the points of intersection of $C(t)$ with S for $t \geq 0$ are precisely the points $C(t_n)$.*

i. If $C(t_1) = C(t_2)$ then $C(t_n) = A$ for all n and C is periodic.

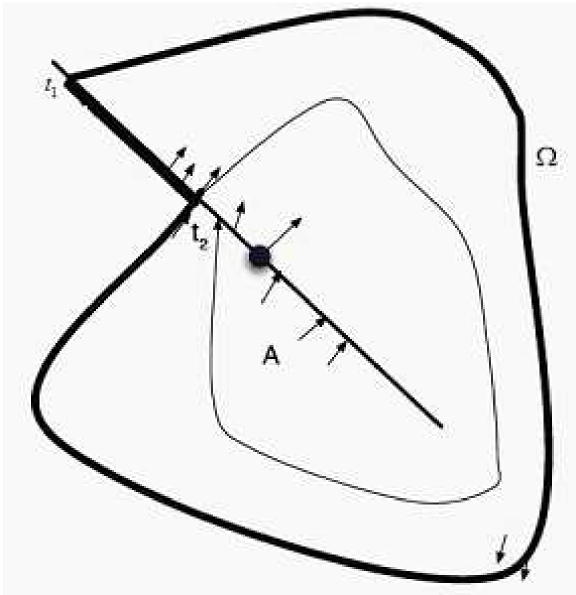

Figure 1: A simple closed curve Ω.

ii. If $C(t_1) \neq C(t_2)$ then all the points $C(t_n)$ are distinct, $C(t_{n+1})$ lies between $C(t_n)$ and $C(t_{n+2})$ on S and the sequence of points $C(t_n)$ converges monotonically on S to A. In particular, $\omega(C) \cap S = \{A\}$. In other words, the transversal S contains only the single point A of $\omega(C)$.

Proof. By definition, every neighborhood of A contains points of the form $C(t)$ with arbitrarily large t. Hence by the preceding lemma, the curve $C(t)$ will cross S infinitely many times with arbitrarily large t. By the lemma 3.10, any finite interval of time contains only finitely many such intersections, and so the intersection times are given by a monotone increasing sequence as stated in the lemma. If $C(t_1) = C(t_2)$ then C is periodic with period $t_2 - t_1$, and by definition the curve C does not cross S at any time between t_1 and t_2. So $C(t_n) = C(t_1)$ and as A is the limit of the $C(t_n)$ (by the preceding lemma) we conclude that $A = C(t_1)$.

Suppose that $C(t_1) \neq C(t_2)$. By definition, C does not intersect S for $t_1 < t < t_2$. So the curve formed by $C(t)$, $t_1 < t < t_2$ and the segment $\overline{C(t_n) \cdot C(s)}$ of S forms a simple closed curve Ω.

We claim that the trajectory $C(t), t > t_2$ cannot cross Ω. Indeed, suppose that $t > t_2$ and close to t_2, then the curve $C(t)$ lies inside Ω. It cannot cross the

C portion of Ω by the uniqueness theorem of ordinary differential equations, and it cannot cross the S portion in the direction opposite to the trajectories at t_1 and t_2. Hence it lies entirely inside Ω for all time. In particular, if $C(t_3)$ is inside Ω and $C(t_2)$ lies between $C(t_1)$ and $C(t_3)$ on S, then by induction $C(t_n)$ form a monotone sequence on S. If the curve starts outside Ω the same argument shows that it must remain outside for all time and the same monotonicity holds. Thus, we complete the proof of the lemma. □

Theorem 3.13. (Pointcare-Bendixsom) *Every nonempty compact $\omega-$limit set in C^1 planar flow that does not contain the equilibrium point is a (non-degenerate) periodic orbit.*

Proof. Let A be a point of $\omega(C)$, D be the trajectory through A and consider $\omega(D)$. Since $\omega(C)$ is closed and since $D(t) \in \omega(C)$ for large t, we conclude that $\omega(D) \subset \omega(C)$. If we suppose that $\omega(C)$ contains no zeros of f, then a point $B \in \omega(D)$ is not a zero of f. Also the set $\omega(D)$ is not empty since the entire forward trajectory through A is bounded, being contained in $\omega(D)$. Choose a transverse segment S through B. By the preceding lemma, S can intersect $\omega(C)$ in only one point. In particular, S can intersect D in at most one point, and hence we conclude that D is periodic. If C is periodic, then we have $C = D$ and the proof of the Poincare-Bendixson theorem is complete.

Now, we construct a forward invariant domain Ω by the planar flow and the corresponding vector field f (see Figure 2) and define arc of circles and segments on the domain. We further define:

$$\omega = -F_\varepsilon(y_w + V) = \frac{-F_0}{1 + |y_w + V|} \tanh\left(\frac{y_w + V}{\varepsilon}\right), for y_w \in (0, \infty). \tag{8}$$

Then, for any fixed ε, if $y_w \to +\infty$,, then $\omega \to 0$.

We then show that for $C(x, y) = (x - x_0)^2 + y^2$, C is decreasing along the orbits $(x, \dot{x}) \Leftrightarrow \forall t \geq 0$ we have

$$\begin{cases} \dot{x}(t) \leq 0, \\ -F_\varepsilon(\dot{x}(t) + V) \geq x_0 \end{cases} or \begin{cases} \dot{x}(t) \geq 0, \\ -F_\varepsilon(\dot{x}(t) + V) \leq x_0 \end{cases}. \tag{9}$$

In fact from Chain Rule,

$$0.5C'(x, \dot{x}) = \dot{x}(x - x_0) + \dot{x}\ddot{x} = \dot{x}(-F_\varepsilon(\dot{x} + V) - x_0).$$

So, we consider an arc C_1 of center $(\omega, 0)$ and radius y_w joining $A_0(a_0, 0)$ and $A_1(a_1, 0)$ where $a_0 = \omega - y_w$ and $a_1 = \omega + y_w$. Then for $M(x, \dot{x}) \in C_1$

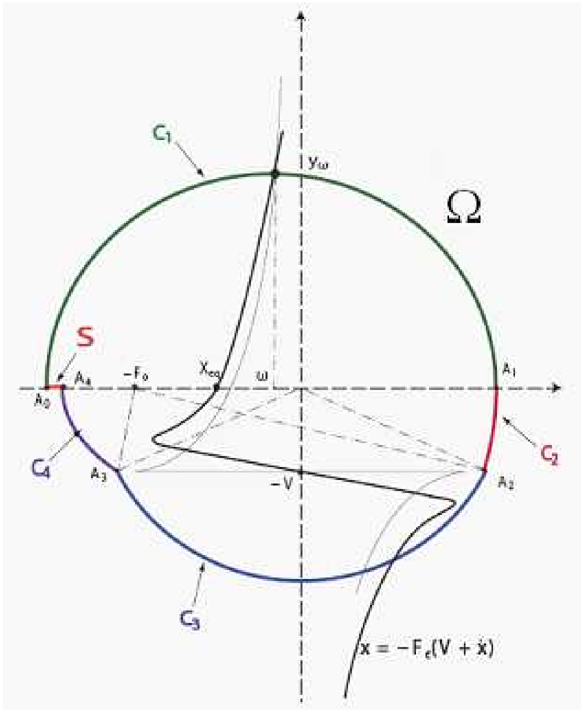

Figure 2: A forward invariant domain Ω.

and $F_\varepsilon(V) > 0$ decreasing in $\mathbb{R}^+$ for $V > V_c$, we have $\dot{x} \geq 0$ and $-F_\varepsilon(\dot{x}+V) \leq -F_\varepsilon(y_w + V) = \omega$. Deducing from the proof of the trajectory property in the phase space with $x_0 = \omega$, it follows that at each point on C_1 the flow goes inside the domain Ω.

Next, let C_2 be an arc length joining $A_1(a_1, 0)$ and $A_2(a_2, -V)$ with center $(-F_0, 0)$ and radius $a_1 + F_0$. Then for $M(x, \dot{x}) \in C_2, \dot{x} \leq 0$ and $-F_\varepsilon(\dot{x}+V) \geq -F_0$. Now, as $x_0 = -F_0$, we have $(a_2+F_0)^2 + V^2 = (a_1+F_0)^2$ and concludes that the flow is entering the domain, Ω. Thus, for large y_w, $(a_1+F_0)^2 - V^2 = (y_w + \omega + F_0)^2 - V^2 \geq 0$ it implies $a_2 = -F_0 + \sqrt{(a_1+F_0)^2 - V^2}$.

Consider arc lengths C_3 and C_4 joining $A_2(a_2, -V)$ and $A_3(a_3, -V)$ with center $(0, 0)$ and $A_3(a_3, -V)$ to $A_4(a_4, 0)$ with center $(-F_0, 0)$ respectively. Then for all $M(x, \dot{x}) \in C_3$ and knowing that $\dot{x} + V \leq 0$, we have $\dot{x} \leq 0$ and $-F_\varepsilon(\dot{x}+V) \geq 0$. Therefore, the flows are entering the domain with $a_3 = -a_2 = F_0 - \sqrt{(a_1+F_0)^2 - V^2} \leq 0$ and $a_4 = -F_0 - \sqrt{(a_3+F_0)^2 + V^2} \leq 0$.

We now consider a segment S joining A_4 and A_0 and show that the domain

Ω enclosed by C_1, C_2, C_3, C_4 and S exhibits forward invariant. In other words, it remains to show that at each point on S, the flow is entering domain Ω. That is, $a_0 \le a_4 \le 0$.

$$\begin{aligned}&a_0 - a_4 = \omega - y_w + F_0 + \sqrt{(a_3+F_0)^2+V^2} \le 0\\ &\Leftrightarrow \sqrt{(a_3+F_0)^2+V^2} \le y_w - \omega - F_0\end{aligned}$$

For large enough y_w such that $y_w - \omega - F_0 \ge 0$ we have

$$\begin{aligned}&a_0 - a_4 \le 0 \Leftrightarrow (a_3+F_0)^2 + V^2 \le (y_w - \omega - F_0)^2,\\ &\Leftrightarrow V^2 + (2F_0 - \sqrt{(a_1+F_0)^2 - V^2})^2 \le (y_w - \omega - F_0)^2,\\ &\Leftrightarrow 4F_0^2 - 4F_0\sqrt{(a_1+F_0)^2-V^2} + (a_1+F_0)^2 \le (y_w - \omega - F_0)^2,\\ &\Leftrightarrow 4F_0^2 - 4F_0\sqrt{(a_1+F_0)^2-V^2} + (y_w+\omega+F_0)^2 \le (y_w - \omega - F_0)^2,\\ &\Leftrightarrow 4F_0^2 - 4F_0\sqrt{(a_1+F_0)^2-V^2} + 4y_w\omega + 4y_wF_0 \le 0,\\ &\Leftrightarrow F_0^2 + y_wF_0 + y_w\omega \le F_0\sqrt{(y_w+\omega+F_0)^2-V^2}.\end{aligned}$$

Since $F_0^2 + y_wF_0 + y_w\omega \ge 0$ for large sufficient y_w, $a_0 - a_4 \le 0$ is true if and only if

$$\begin{aligned}&(F_0^2 + y_w(F_0+\omega))^2 \le F_0^2((\omega + y_w + F_0)^2 - V^2)\\ &\Leftrightarrow F_0^4 + 2F_0^2(F_0+\omega)y_w + (F_0+\omega)^2y_w^2 \le F_0^4 + 2F_0^3(y_w+\omega)\\ &+F_0^2(y_w+\omega)^2 - F_0^2V^2,\\ &\Leftrightarrow F_0^2V^2 \le F_0^2\omega^2 + 2F_0^3\omega - 2F_0\omega y_w^2 - \omega^2y_w^2 = +\infty,\end{aligned}$$

Since $\lim\limits_{y_w\to\infty} \omega = 0$, $\lim\limits_{y_w\to\infty} \omega y_w = -F_0$, $\lim\limits_{y_w\to\infty} \omega^2 y_w^2 = F_0^2$, $\lim\limits_{y_w\to\infty} \omega y_w^2 = -\infty$, there exists y_w large enough that

$$F_0^2\omega^2 + 2F_0^3\omega - 2F_0\omega y_w^2 - \omega^2y_w^2 \ge F_0^2V^2.$$

Thus, we can choose $y_w \in (0,\infty)$ in such a way that $a_0 \le a_4$. Therefore, for a certain y_w, the domain Ω is a forward invariant.

Assuming a compact forward invariant domain Ω, the ω -limit set of any point in Ω is a compact contained in Ω. Since our equilibrium point $X_e = (-F_e(V), 0)$ is unique for $V > V_c$, we expect that every other ω -limit set (except X_e) would be periodic orbit. □

4. Local and Global Existence of Weakly Coupled problem

Next, we prove that for a small perturbation (i.e. ℓ close to zero), there exists a periodic solution to equation (2).

Theorem 4.1. *For $\ell \approx 0$, there exists a periodic orbit of equation (2) close to x_0, with the same time period T_0, and inverse velocity τ close to τ_0, such that x_0 is non-degenerate.*

Proof. Consider a system where the blocks were coupled with a finite number of other masses in the form:

$$\frac{\dot{X}_n(t)}{\tau} = H(X(t)) + \ell^2 \sum_{k\in K} \psi_k T_k X(t), \tag{10}$$

where $X(t) \in \mathbb{R}^d, T_k X(t) = X(t-k), and H$ and ψ_k representing smooth functions from $\mathbb{R}^d into \mathbb{R}^d$ and K is a finite set. For example, in the rate and state case we have

$$X(t) = \left(\begin{array}{c} x(t) \\ \frac{1}{\tau}\dot{x}(t) \\ \theta(t) \end{array} \right)$$

which satisfies

$$\frac{\dot{X}(t)}{\tau} = H(X(t)) + \ell^2 \sum_{k\in K} \left(\begin{array}{c} 0 \\ \psi_k T_k x(t) \\ 0 \end{array} \right). \tag{11}$$

So, we can hypothesize that:

i. For $\ell = 0$ there exist a T_0-periodic solution X_0 such that for any $\tau = \tau_0 \in \mathbb{R}^+$, X_0 is a solution of $\frac{\dot{X}}{\tau_0} = H(X)$ and

ii. One is a simple Floquent multiplier for the linearized equation $\frac{\dot{X}}{\tau_0} = DH(X_0)X$.

The existence of the first part of hypothesis (i) is verified in Theorem 3.4 while the stability of the periodic orbit discussion in theorem 4.2 proves the second part of the hypothesis. □

Theorem 4.2. *Suppose the hypothesis above is satisfied for (X_0, τ_0, T_0). Then there exist neighborhoods $\gamma \in \mathbb{R}$ and $\varphi \in (X_0, \tau_0)$ in $H^2(\mathbb{R}/T_0, \mathbb{R}) \times H^1(\mathbb{R}/T_0, \mathbb{R}) \times H^1(\mathbb{R}/T_0, \mathbb{R}) \times \mathbb{R}$, such that for all $\ell \in \gamma$, there exists a T_0-periodic solution of (11), $X(\ell)$ traveling at velocity $\tau(\ell)^{-1} \in \varphi$ which is unique up to phase shift.*

Proof. Since there exists an advance-and-delay term in our model equation, we search for X with the same period T_0 as X_0 by fixing T_0 and considering a small perturbation $X = X_0 + X_1$ with velocity τ^{-1}, where $X_1 = (x_1, v_1, \theta_1)$ and $v_1 = \tau^{-1}\dot{x}_1$. Substituting $X = X_0 + X_1$ into (11) gives

$$\frac{\dot{X}_0 + \dot{X}_1}{\tau} = H(X_0 + X_1) + \ell^2 \sum_{k\in K} \begin{pmatrix} 0 \\ \psi_k T_k(x_0 + x_1) \\ 0 \end{pmatrix}. \tag{12}$$

Thus we can rewrite (12) as

$$\hbar(X_1, \tau, \ell) = -\frac{\dot{X}_0 + \dot{X}_1}{\tau} + H(X_0 + X_1) + \ell^2 \sum_{k\in K} \begin{pmatrix} 0 \\ \psi_k T_k(x_0 + x_1) \\ 0 \end{pmatrix} = 0. \tag{13}$$

Since $D\hbar(0, \tau_0, 0)$ is not invertible in the neighborhood of $(0, \tau_0, 0)$ we could not use the Implicit Function Theorem to solve (12). Rather, we follow Lyaponov-Schmidt method which transforms the equation into a well defined space.

Assuming a linear operator $\wp$ from $E \in H^2(\mathbb{R}/T_0, \mathbb{R}) \times H^1(\mathbb{R}/T_0, \mathbb{R}) \times H^1(\mathbb{R}/T_0, \mathbb{R})$ into $F \in L^2(\mathbb{R}/T_0, \mathbb{R}^3)$ and define

$$\begin{cases} \wp(X_1) = D_{U_1}\hbar(0, \tau_0, 0) \cdot X_1, \\ N(X_1, \tau, \ell) = \wp(X_1) - \hbar(X_0, \tau, \ell) \end{cases} \tag{14}$$

Then,

$$\begin{aligned} \wp(X_1) &= -\tau_0^{-1}\dot{X}_1(\tau_0) + DH(X_0) \cdot X_1 \\ &= \begin{pmatrix} 0 \\ -\frac{1}{\tau_0^2}\ddot{x}_1 + D_1F(x_0, \frac{1}{\tau_0}\dot{x}_0, \theta_0)x_1 + \frac{1}{\tau_0}D_2F(x_0, \frac{1}{\tau_0}\dot{x}_0, \theta_0)\dot{x}_1 \\ +D_3F(x_0, \frac{1}{\tau_0}\dot{x}_0, \theta_0)\theta_1 \\ -\frac{1}{\tau_0}\dot{\theta}_1 + D_1\hbar(x_0, \frac{1}{\tau_0}\dot{x}_0, \theta_0)x_1 + \frac{1}{\tau_0}D_2\hbar(x_0, \frac{1}{\tau_0}\dot{x}_0, \theta_0)\dot{x}_1 \\ +D_3\hbar(x_0, \frac{1}{\tau_0}\dot{x}_0, \theta_0)\theta_1 \end{pmatrix}, \end{aligned} \tag{15}$$

where D_i denotes the derivative with respect to the i-th variable. Let define a kernel of $\wp$ by $N(\wp_{|E})$ and denote the range of $\wp$ by $R(\wp_{|E})$ then $\hbar(X_1, \tau, \ell) = 0$ can be written as

$$\wp(X_1) = N(X_1, \tau, \ell). \tag{16}$$

For L in F,

i. $N(\wp_{|E}) = span(\dot{X}_0)$

ii. $L \in R(\wp_{|E}) \Leftrightarrow \exists X \in E, \frac{1}{\tau_0}\dot{X} - DH(X_0) \cdot X = L \Leftrightarrow \exists X \in E, \dot{X} - A(t)X = \tau_0 L(t)$,

where $A(t) = \tau_0 DH(X_0))$ is a T_0-periodic matrix. □

Lemma 4.3. *The range of $\wp_{|E}$ is of codimension one and is given by $R(\wp_{|E})$
$= (span\psi_0)^{\perp}$, where ψ_0 is a T_0-periodic solution of the adjoint equation.*

Remark 4.4. The Lemma follows directly from Fredholm's Alternative which is stated as proposition 4.5 below.

Proposition 4.5. *Consider non homogeneous equation:*

$$\dot{x} = A(t)x + f(t), \tag{17}$$

Where $A(t)$ is the matrix of an endomorphism A on $\mathbb{C}^n$, such that A is continuous and T-periodic and $f(t)$ is a T-periodic application from $\mathbb{R} into \mathbb{C}^n$. Then there exists a T-periodic solution of equation (17) if and only if the compatibility condition (18) is satisfied

$$\int_0^T \langle y(t), f(t)\rangle_{\mathbb{C}^n}\, dt = 0, \tag{18}$$

for all y such that it is a T-periodic solution of the adjoint equation (19),

$$\dot{z} = -zA(t). \tag{19}$$

In addition, the space of T-periodic solutions of (19) has the same dimension as the space of T-periodic solutions of the homogeneous equation (17).

Remark 4.6. Proposition 4.5 gives existence of periodic solution for a non homogeneous periodic equation provided that the compatibility condition (17) is satisfied. Let ψ_0 be a T_0-periodic function from $\mathbb{R}$ to $\mathbb{R}^3$ whose solution satisfies equation (18), then ψ_0 spans the space of T_0-periodic solutions to (18) in 3 dimensions. That is $R(\wp_{|E}) = span(\psi_0)^{\perp}$ where $\perp$ represents orthogonality for the scalar product in:

$$L^2_{T_0}(\mathbb{R}, \mathbb{R}^3) : \langle f, \hbar\rangle_{L^2_{T_0}(\mathbb{R},\mathbb{R}^3)} = \int_0^T \langle f(t), \hbar(t)\rangle_{\mathbb{R}^3}\, dt.$$

Projecting equation (16) onto $span\psi_0 and (span\psi_0)^{\perp}$, we decompose $X_1 = \bar{X}_1 + a\dot{X}_0$ to obtain

$$\wp(X_1) = \prod N(\bar{X}_1 + a\dot{X}_0, \tau, \ell), \tag{20}$$

$$0 = (Id - \prod)N(\bar{X}_1 + a\dot{X}_0, \tau, \ell), \tag{21}$$

where $a \in \mathbb{R}, \bar{X}_1 \in (span\ \dot{X}_0)^{\perp}$ and $\prod$ is the orthogonal projection onto $R(\wp)$.

We can solve equation (20) in the neighborhood of $(0, \tau_0, 0)$ by the Implicit Function Theorem, since $\wp$ is isomorphism from $span(\dot{X}_0)^{\perp}$ into $R(\wp)$ and $D_{X_1}N(0, \tau_0, 0) \cdot X_1 = 0$. Thus, X_1 is obtained as

$$\begin{cases} \bar{X}_1 = \bar{X}_1^*(a, \tau, \ell) \\ \bar{X}_1^*(0, \tau_0, 0) = 0 \end{cases}$$

Therefore in the neighborhood of $(\bar{X}_1, a, \tau, \ell) = (0, 0, \tau_0, 0)$, we write:

$$X_1 = \bar{X}_1^*(a, \tau, \ell) + a\dot{X}_0. \tag{22}$$

To resolve the bifurcation equation (21), we note that $(Id - \prod)$ is the orthogonal projection onto $span\psi_0$,. Thus equation (21) can be written as

$$\begin{aligned} &(Id - \textstyle\prod_1)N(\bar{X}_1^*(a, \tau, \ell) + a\dot{X}(0, \tau, \ell)) = 0 \\ &\Leftrightarrow \left\langle N(\bar{X}_1^* + a\dot{X}_0), \psi_0 \right\rangle_{L^2_{T_0}(\mathbb{R}, \mathbb{R}^3)} = 0 \\ &\Leftrightarrow \textstyle\int_0^{T_0} \left\langle N(\bar{X}_1^* + a\dot{X}_0), \psi_0 \right\rangle_{\mathbb{R}^3} dt = 0 \end{aligned} \tag{23}$$

Thus, solving for N gives

$$N(X_1, \tau, \ell) = \wp(X_1) - \hbar(X_1, \tau, \ell). \tag{24}$$

Therefore, from equation (13), N reads

$$\begin{aligned} N(X_1, \tau, \ell) = \tfrac{\dot{X}_0}{\tau} + &\begin{pmatrix} \dot{x}_1\tau^{-1} \\ \dot{x}_1\tau^{-2} \\ \dot{\theta}_1\tau^{-1} \end{pmatrix} - \begin{pmatrix} (\dot{x}_0 + \dot{x}_1)\tau^{-1} \\ F(x_0 + x_1, (\dot{x}_0 + \dot{x}_1)\tau^{-1}, \theta_0 + \theta_1) \\ G(x_0 + x_1, (\dot{x}_0 + \dot{x}_1)\tau^{-1}, \theta_0 + \theta_1) \end{pmatrix} \\ -\ell^2 \textstyle\sum_{k \in K} &\begin{pmatrix} 0 \\ \psi_k T_k(x_0 + x_1) \\ 0 \end{pmatrix} \\ + &\begin{pmatrix} 0 \\ -\frac{1}{\tau_0^2}\ddot{x}_1 + D_1F(x_0, \frac{1}{\tau_0}\dot{x}_0, \theta_0)x_1 + \frac{1}{\tau_0}D_2F(x_0, \frac{1}{\tau_0}\dot{x}_0, \theta_0)\dot{x}_1 \\ +D_3F(x_0, \frac{1}{\tau_0}\dot{x}_0, \theta_0)\theta_1 \\ -\frac{1}{\tau_0}\dot{\theta}_1 + D_1\hbar(x_0, \frac{1}{\tau_0}\dot{x}_0, \theta_0)x_1 + \frac{1}{\tau_0}D_2\hbar(x_0, \frac{1}{\tau_0}\dot{x}_0, \theta_0)\dot{x}_1 \\ +D_3\hbar(x_0, \frac{1}{\tau_0}\dot{x}_0, \theta_0)\theta_1 \end{pmatrix}. \end{aligned}$$

Denoting $C(a,\tau,\ell) = \left\langle N(X_1^* + a\dot{X}_{0,\tau,\ell}), \psi_0 \right\rangle_{L^2_{T_0}(\mathbb{R},\mathbb{R}^3)}$ $andc(\tau) = C(0,\tau,0)$, we have

$$c(\tau) = \left\langle \dot{X}_0\tau^{-1} + \begin{pmatrix} -\dot{x}_0 \\ (\tau^{-2}-\tau_0^{-2})\ddot{\bar{x}}_1^*(0,\tau,0) + D_1F\bar{x}_1^* + \tau_0^{-1}D_2F\dot{\bar{x}}_1^* \\ +D_3F\bar{\theta}_1^* - F(x_0+\bar{x}_1^*, \tau^{-1}(\dot{x}_0+\bar{x}_1^*), \theta_0+\bar{\theta}_1^* \\ (\tau^{-1}-\tau_0^{-1})\dot{\bar{\theta}}_1^*(0,\tau,0) + D_1G\bar{x}_1^* + \tau_0^{-1}D_2G\dot{\bar{x}}_1^* \\ +D_3G\bar{\theta}_1^* - G(x_0+\bar{x}_1^*, \tau^{-1}(\dot{x}_0+\bar{x}_1^*), \theta_0+\bar{\theta}_1^* \end{pmatrix}, \psi_0 \right\rangle, \tag{25}$$

where the differentials of F and G are taken at $X_0 = (x_0, \tau_0^{-1}\dot{x}_0, \theta_0)$. Hence,

$$\dot{c}(\tau) = \left\langle -\tau^{-2}\dot{X}_0, \psi_0 \right\rangle + \langle d(\tau), \psi_0 \rangle \tag{26}$$

where $d(\tau) = \begin{pmatrix} d_1(\tau) \\ d_2(\tau) \\ d_3(\tau) \end{pmatrix}$ are given below and the differential in $FandG$ are taken at X_0.

$$d_1(\tau) = \tau^{-2}\dot{x}_0,$$

$$\begin{aligned} d_2(\tau) &= -2\tau^{-3}\ddot{\bar{x}}_1^* + (\tau^{-2}-\tau_0^{-2})\tfrac{\partial\ddot{\bar{x}}_1^*}{\partial\tau} + D_1F\tfrac{\partial\bar{x}_1^*}{\partial\tau} + \tau_0^{-1}D_2F\tfrac{\partial\dot{\bar{x}}_1^*}{\partial\tau} + D_3F\tfrac{\partial\bar{\theta}_1^*}{\partial\tau} \\ &-D_1F(x_0+\bar{x}_1^*, \tau^{-1}(\dot{x}_0+\dot{\bar{x}}_1^*), \theta_0+\bar{\theta}_1^*)\cdot\tfrac{\partial\bar{x}_1^*}{\partial\tau} \\ &-D_2F(x_0+\bar{x}_1^*, \tau^{-1}(\dot{x}_0+\dot{\bar{x}}_1^*), \theta_0+\bar{\theta}_1^*)\cdot\left\{-\tau^{-2}(\dot{x}_0+\dot{\bar{x}}_1^*) + \tau^{-1}\tfrac{\partial\dot{\bar{x}}_1^*}{\partial\tau}\right\} \\ &-D_3F(x_0+\bar{x}_1^*, \tau^{-1}(\dot{x}_0+\dot{\bar{x}}_1^*), \theta_0+\bar{\theta}_1^*)\cdot\tfrac{\partial\bar{\theta}_1^*}{\partial\tau}, \end{aligned}$$

$$\begin{aligned} d_3(\tau) &= -\tau^{-2}\dot{\bar{\theta}}_1^* + (\tau^{-1}-\tau_0^{-1})\tfrac{\partial\dot{\bar{\theta}}_1^*}{\partial\tau} + D_1G\tfrac{\partial\bar{x}_1^*}{\partial\tau} + \tau_0^{-1}D_2G\tfrac{\partial\dot{\bar{x}}_1^*}{\partial\tau} + D_3G\tfrac{\partial\bar{\theta}_1^*}{\partial\tau} \\ &-D_1G(x_0+\bar{x}_1^*, \tau^{-1}(\dot{x}_0+\dot{\bar{x}}_1^*), \theta_0+\bar{\theta}_1^*)\cdot\tfrac{\partial\bar{x}_1^*}{\partial\tau} \\ &-D_2G(x_0+\bar{x}_1^*, \tau^{-1}(\dot{x}_0+\dot{\bar{x}}_1^*), \theta_0+\bar{\theta}_1^*)\cdot\left\{-\tau^{-2}(\dot{x}_0+\dot{\bar{x}}_1^*) + \tau^{-1}\tfrac{\partial\dot{\bar{x}}_1^*}{\partial\tau}\right\} \\ &-D_3G(x_0+\bar{x}_1^*, \tau^{-1}(\dot{x}_0+\dot{\bar{x}}_1^*), \theta_0+\bar{\theta}_1^*)\cdot\tfrac{\partial\bar{\theta}_1^*}{\partial\tau}. \end{aligned}$$

For $\tau = \tau_0$, we have $\bar{x}_1^*(0,\tau_0,0) = \dot{\bar{x}}_1^*(0,\tau_0,0) = 0$. Thus

$$\begin{aligned} \dot{c}(\tau_0) &= \left\langle -\tau_0^{-2}\dot{X}_0 + \begin{pmatrix} \tau_0^{-2}\dot{x}_0 \\ \tau_0^{-2}D_2F(x_0,\tau_0^{-1}\dot{x}_0,\theta_0)\dot{x}_0 \\ \tau_0^{-2}D_2G(x_0,\tau_0^{-1}\dot{x}_0,\theta_0)\dot{x}_0 \end{pmatrix}, \psi_0 \right\rangle, \\ &= \left\langle -\tau_0^{-1}\left[\tau_0^{-1}\dot{X}_0 - \begin{pmatrix} 0 & 1 & 0 \\ 0 & D_2F(x_0,\tau_0^{-1}\dot{x}_0,\theta_0) & 0 \\ 0 & D_2G(x_0,\tau_0^{-1}\dot{x}_0,\theta_0) & 0 \end{pmatrix}\cdot X_0\right], \psi_0 \right\rangle. \end{aligned} \tag{27}$$

Lemma 4.7. *Under our hypothesis we conclude that* $\dot{c}(\tau_0) \neq 0$.

Proof. Let assume that $\dot{c}(\tau_0) = \frac{\partial C(0,\tau_0,0)}{\partial \tau} = 0$, then the compatibility condition (18) in Proposition 4.5 for the following equation is satisfied

$$\tau_0^{-1}\dot{X} - DH(X_0)\cdot X = \tau_0^{-1}\dot{X}_0 - \begin{pmatrix} 0 & 1 & 0 \\ 0 & D_2F(x_0, \tau_0^{-1}\dot{x}_0, \theta_0) & 0 \\ 0 & D_2G(x_0, \tau_0^{-1}\dot{x}_0, \theta_0) & 0 \end{pmatrix} \cdot X_0.$$

Considering $\xi_0(t) = X_0(t\tau_0) and \xi(t) = X(t\tau_0)$, we have

$$\dot{\xi} - DH(\xi_0)\cdot\xi = \dot{\xi}_0 - \begin{pmatrix} 0 & 1 & 0 \\ 0 & D_2F(x_0, \dot{x}_0, \psi_0) & 0 \\ 0 & D_2G(x_0, \dot{x}_0, \psi_0) & 0 \end{pmatrix} \cdot \xi_0 = \dot{\xi}_0 - DH(\xi_0)\cdot \begin{pmatrix} 0 \\ \dot{x}_0 \\ 0 \end{pmatrix}.$$

This satisfies a T-Periodic solution, $\xi^* = (x^*, \dot{x}^*, \theta_x^*)$, with $T = \tau_0 T_0$. Let $Z = \xi^* - \begin{pmatrix} 0 \\ \dot{x}_0 \\ 0 \end{pmatrix}$, then Z satisfies $\dot{Z} = \begin{pmatrix} \dot{x}^* \\ \ddot{x}^* - \ddot{x}_0 \\ \dot{\theta}_x^* \end{pmatrix}$

$$= \begin{pmatrix} \dot{x}^* \\ D_1F(\xi_0)x^* + D_2F(\xi_0)\dot{x}^* + D_3F(\xi_0)\theta_x^* + \ddot{x}_0 - D_2F(\xi_0)\dot{x}_0 \\ D_1G(\xi_0)x^* + D_2G(\xi_0)\dot{x}^* + D_3G(\xi_0)\theta_x^* + \dot{\theta}_0 - D_2G(\xi_0)\dot{x}_0 \end{pmatrix}$$

$$\dot{Z} = DH(\xi_0)\cdot Z + \dot{\xi}_0. \tag{28}$$

Since $\dot{\xi}_0$ is the solution of the linearized equation $\tau_0^{-1}\dot{X} = DH(X_0)X$ in our hypothesis, the solutions of equation (28) will be of the form

$$Z(t) = R(t)Z_0 + t\dot{\xi}_0(t), \tag{29}$$

where $R(t)$ is the fundamental matrix of the equation $\tau_0^{-1}\dot{X} = DH(X_0)X$.

If Z is the T-Periodic solution of (28), then

$$Z(T) = Z(0) = Z_0 = R(t)Z_0 + T\dot{\xi}_0(T) \tag{30}$$

$$\Leftrightarrow R(t)Z_0 = Z_0 - T\dot{\xi}_0(T) = Z_0 - T\dot{\xi}_0(0). \tag{31}$$

However, Z_0 and $\dot{\xi}_0(0)$ are linearly independent in $\mathbb{R}^3$. Assuming they are not, then there exists a $\mu \in \mathbb{R}$, such that $Z_0 = \mu\dot{\xi}_0(0)$. Thus, equation (30) becomes

$$Z(T) = Z_0 = \mu\dot{\xi}_0(0) = \mu R(t)\dot{\xi}_0(0) + T\dot{\xi}_0(0). \tag{32}$$

So, $\dot{\xi}_0$ is a T-Periodic solution of equation $\tau_0^{-1}\dot{X} = DH(X_0)X$. Implying

$$R(T)\cdot\dot{\xi}_0(0) = \dot{\xi}_0(T) = \dot{\xi}_0(0), \tag{33}$$

which reduces equation (32) to

$$\mu\dot{\xi}_0(0) = \mu\dot{\xi}_0(0) + T\dot{\xi}_0(0) \tag{34}$$

Hence, it follows that $T = 0$, which is a contradiction. Therefore, 1 is not a simple Floquet multiplier which contradicts our hypotheses. That proves Lemma 4.6. □

To conclude the proof of Theorem 4.2, we notice that equation (21) is equivalent to $C(a, \tau, \ell) = 0$. So by using Lemma 4.6, we can solve equation (21) with the Implicit Function Theorem since $\dot{c}(\tau_0) \neq 0$. Thus, in the neighborhood of $\gamma(0, \tau_0, 0)$, we have

$$C(a, \tau, \ell) = 0 \Leftrightarrow \tau = \tau^*(a, \ell) with \tau^*(0, 0) = \tau_0.$$

Implying, $X = \bar{X}_1^*(a, \tau^*(a, \ell), \ell) + a\dot{X}_0$.

This means that for all ℓ near zero, there exists a unique one parameter family, $\{(X(t, a, \ell), \tau(a, \ell), a \in \gamma(0)\}$, of T-Periodic solutions of (11) in the neighborhood of (X_0, τ_0).

5. Numerical Simulation and Analysis

We simulate equation (2) numerically with a Runge-Kutta method for fixed time step of 0.05 to investigate the effect of varying ℓ and visually tracing the motion of the system as ℓ increases. The time step is chosen just small enough to balance sufficient time resolution and reasonable computational cost. The simulation uses 10,000 blocks and at least 50,000 events with a small spatial perturbation of amplitude 0.001. The ratio of the spring to leaf spring stiffness, ℓ, controlled the proportion of small to large events. As ℓ approaches infinity, we expect the chain of blocks to be rigid bar and all events becoming system wide events. Similarly as ℓ approaches 0, we expect each individual block to move independently and all events becoming single block events.

In other words, the strain energy available for any block through the leaf spring is inversely proportional to the leaf spring stiffness. So, as the leaf spring stiffness goes to zero, the available strain energy becomes very large, leading to very large events. Similarly, as the leaf spring stiffness goes to infinity, the available strain energy through the leaf spring becomes infinitely small, leading to single block events. Thus, we could expect an increase in the number of large events as the stiffness ratio ℓ is increased, (see Figure 3). In this figure, the cumulative size distribution was plotted against the event length. One

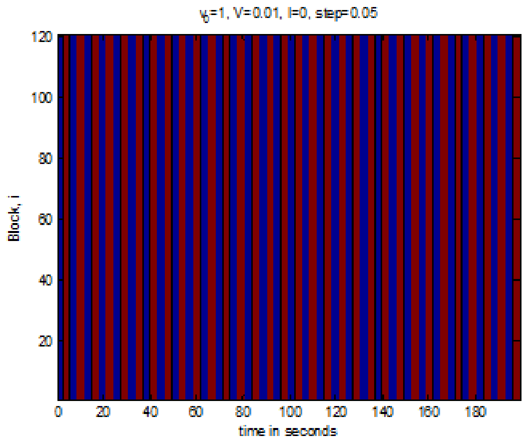

Figure 3: $\ell = 0$, corresponds to the single block periodic motion which are essentially the same in both limits.

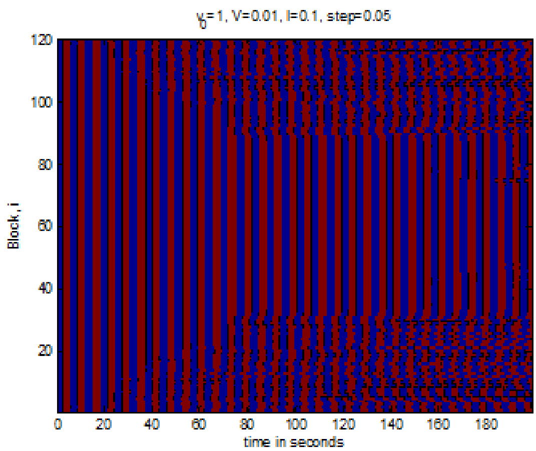

Figure 4: For small ℓ, the motion of each block is periodic, but the small coupling with the rest of the system rendered an alternative pattern. We also observed a certain amount of solitonic activity where small fractures propagated in both directions.

advantage of using cumulative distribution was that it depicts how the slopes of the linear part of the distributions reflect to each other for different ℓ. We observed that the linear part became steeper as ℓ decreased which implied an increased in proportion of small events.

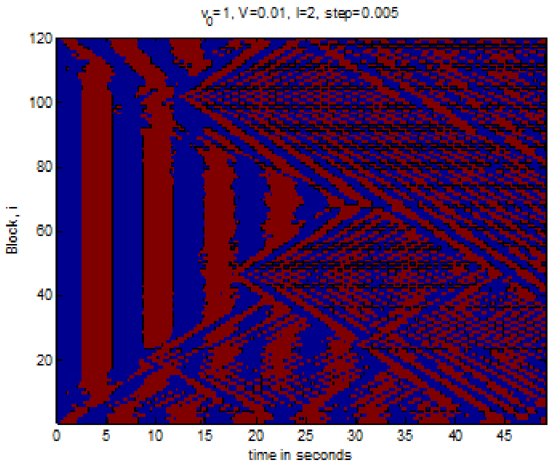

Figure 5: For $\ell = 2$, A unique characteristics where the solitons ran through the whole system was observed.

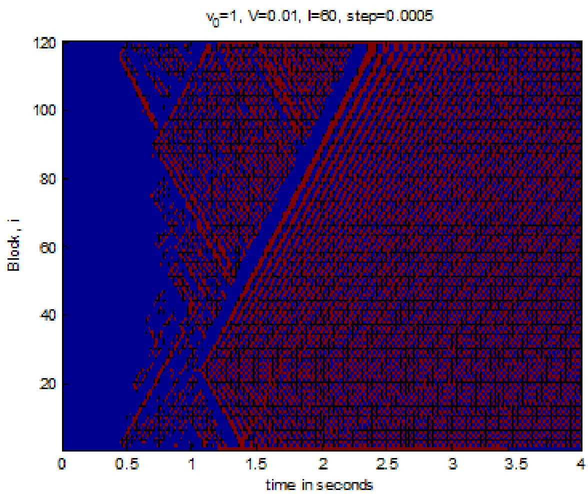

Figure 6: In the case for $\ell = 60$, we observed solitons producing approximately two turns in the system before decaying.

Figures 4-7 present the result for the average friction force plotted as a function of the dimensionless pulling velocity for different values of ℓ. The red lines or dots represented the particle i that is moving at time t. The transition as ℓ increase is a three step transition: from free motion to cooperative motion then

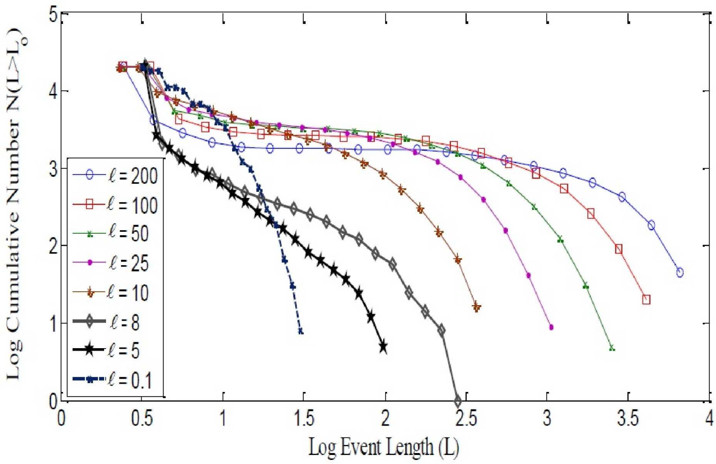

Figure 7: Cumulative distribution of event lengths for different values ℓ. The vertical axis represents log of the number of events having a length greater than a given value, whereas the horizontal axis depicts the size of the event measured by log the number of blocks which have moved in that event. As ℓ is increased, the distribution changes from one which is dominated by small events ($\ell = 0$) to distribution dominated by increased proportion of large events. Also, the slopes of the linear part in different curves increased as ℓ is reduced, reflecting an increase in the number of small events.

to rigid motion. For $\ell = 0$, the periodicity of each block was translated into a periodic pattern for the velocity of the center of mass (see Figure 4). Transition as ℓ increases are depicted in Figures 5 and 6. For small $\ell = 0.01$, the motion for each individual block was also periodic, but the small coupling rendered an alternating pattern as shown in Figure 5. As ℓ increased we observed that there existed a certain amount of solitonic activity where small fractures propagated in both directions. For $\ell = 2$, a qualitatively distinct pattern where the solitons ran through the whole system was observed, as shown in Figure 6. Further investigation revealed that for $\ell = 60$, a solitary wave which divided into approximately two turns to the chain before finally decaying was observed. This observation confirmed Schmittbuhl et al. (1993) article about the existence of two solitary waves in spring-block propagative modes.

6. Conclusion

The local and global existence of wave solutions under which a spring-block model coupled with smooth fiction were studied and proved analytically. We then investigated the influence of the parameter ℓ in the motion of the spring-block model. We observed that varying ℓ created an interval of solitonic wave activity between two values of $\ell = 0$ and ℓ large. For $\ell = 0$ or ℓ large, the blocks in the chain moved periodically while the blocks exhibited more complex characteristics in between $\ell = 0$ and ℓ large. Such behavior is characterized by the appearance of propagating fractures at speed slightly larger than the speed of sound. Thus, it was in this range of values of ℓ where chaotic motions were observed for small values of V. Both analytical and numerical solutions provided insight to solitary waves and may help provide more understanding of earthquakes and other dissipative driven systems.

References

[1] P. Segall, E.K. Desmarais, D. Shelly, A. Miklius, P. Cervelli, Earthquakes triggered by silent slip events on K'lauea volcano, *Hawaii. Natur*, **442** (2006), 71-74.

[2] R.B. Lohman, J.J. Mc Guire, Earthquake swarms driven by aseismic creep in the Salton Trough, *California. J. Geophys. Res.*, **112** (2007), B04405.

[3] Y. Liu, J.R. Rice, K.M. Larson, Seismicity variations associated with aseismic transients in Guerrero, Mexico, 1995-2006, *Earth Planet. Sci. Lett.*, **262** (2007), 493- 504.

[4] Y. Takada, M. Furuya, Aseismic slip during the 1996 earthquake swarm in and around the Onikobe geothermal area, *NE Japan. Earth Planet. Sci. Lett.*, **290** (2010), 302-310.

[5] S. Bourouis, P. Bernard, Evidence for coupled seismic and asei smic fault slip during water injection in the geothermal site of Soultz (France), and implications for seismogenic transients, *Geophys. J. Int.*, **169** (2007), 723-732.

[6] C.H. Scholz, *The Mechanics of Earthquakes and Faulting*, Second Ed., Cambridge University Press, New York (2002), 496pp.

[7] R. Burridge, L. Knopoff, Model and theoretical seismicity, *Bull. Seismol. Soc. Amer.*, **57** (1967), 341.

[8] J.M. Carlson, J.S. Langer, Properties of earthquakes generated by fault dynamics, *Phys. Rev. Lett.*, **68** (1989), 2632.

[9] J. Schmittbuhl, J.P. Vilotte, S. Roux, Propagative macro-dislocation modes in earthquake fault model, *Europhysics Letters*, **1** (1993), 375-380.

[10] C. Marone, Laboratory-derived friction laws and their application to seismic faulting, *Annu. Rev. Earth Planet. Sci.*, **26** (1998), 643-696.

[11] N. Lapusta, J.R. Rice, Nucleation and early seismic propagation of small and large events in a crustal earthquake model, *J. Geophys. Res.*, **108** (2003), 1-18.

[12] E.G. Daub, J.M. Carlon, A constitutive model for fault gouge deformation in dynamic rupture simulations, *J. Geophys. Res.* (2007).

[13] J.M. Carlson, J.S. Langer, Mechanical model of an earthquake fault, *Phys. Rev. A* , **40** (1989), 6470-6484.

[14] J.M. Carlson, J.S. Langer, Properties of earthquakes generated by fault dynamics, *Phys. Rev. Lett.*, **62** (1989), 2632-2635.

[15] J.S. Langer, C. Tang, Rupture propagation in a model of an earthquake fault, *Phys Rev Lett.*, **67**, No. 8 (1991), 1043-1046.

[16] G. Iooss, M. Adelmeyer, *Topics in Bifurcation Theory and Applications*, World Scientific (1998).